energy&fuels

Article

pubs.acs.org/EF

Shock Tube and Kinetic Modeling Study of Isobutanal Oxidation

Jiaxiang Zhang, Lun Pan, Zihang Zhang, Jun Mo, and Zuohua Huang*

State Key Laboratory of Multiphase Flow in Power Engineering, Xi'an Jiaotong University, Xi'an 710049, People's Republic of China

Supporting Information

ABSTRACT: Optimization of chemical kinetic modeling for biobutanol oxidation requires further investigation on its key stable intermediates, such as aldehydes. In this study, ignition delay times of isobutanal/oxygen diluted with argon were measured behind reflected shock waves in the temperature range of 1100−1650 K, at pressures of 1.3, 5, and 10 atm, and equivalence ratios of 0.5, 1.0, and 2.0. An isobutanal submodel was developed on the basis of literature review, and it yields fairly good agreement with the experimental results under the test conditions. The reaction pathway and sensitivity analysis were performed to gain insight into the controlling reaction pathways and reaction steps.

1. INTRODUCTION

Biobutanol is considered to be a promising fuel with some advantages.[1,2] In comparison to *n*-butanol, isobutanol has a higher octane number. It has been used as an additive to gasoline[3−6] and diesel[7,8] engines. Some fundamental studies[9−17] have been performed on isobutanol, with several chemical mechanisms proposed.[11,12,15−17] As the kinetic modeling of butanols is becoming more mature, special attention should be paid on the chemical kinetics of the stable intermediates, such as aldehydes. Isobutanal was identified as a key stable intermediate during the oxidation of isobutanol.[10,12,13] Welz et al.[13] studied the low-temperature oxidation of isobutanol using multiplexed time-resolved tunable synchrotron photoionization mass spectrometry. They found that the $(CH_3)_2CHCHOH + O_2$ reaction primarily forms isobutanal and HO_2 radicals via direct HO_2 elimination, which is a major difference between the low-temperature chemistry of alkanes and alcohols. At high temperatures, isobutanal is mainly produced through decomposition of the radicals that result from the H-abstraction at the α-carbon site or the hydroxyl group. Being an essential part of the isobutanol mechanism, the oxidation of isobutanal is worth being investigated.

Some experimental and theoretical studies have been conducted on the oxidation of small aldehydes, such as formaldehyde[18−20] and acetaldehyde.[21−23] There were also a few reports on the study of oxidation for the larger aldehyde, propanal.[24−32] Most of the earlier studies focused on its negative temperature coefficient (NTC) behavior. Some recent studies were carried out using shock tube,[28,29] flame,[30,31] and jet-stirred reactor (JSR)[32] experiments. Lifshitz et al.[28] studied the decomposition of propanal behind reflected shock waves for temperatures ranging from 970 to 1300 K. They proposed a detailed chemical kinetic model, which consists of 22 species and 52 elementary reactions. Akih-Kumgeh et al.[29] measured the high-temperature ignition delay times for propanal behind reflected shock waves at elevated pressures. A chemical kinetic model was developed and yielded fairly good agreement with the experimental results. Kasper et al.[30] measured the stable intermediate species and radicals in low-pressure, burner-stabilized, premixed stoichiometric propanal flames. Their observation suggested that the majority of oxygenated intermediates with high molecular weights were formed by the addition of an alkyl radical to the aldehyde fuel. Burluka et al.[31] measured the laminar flame speeds of three C_3H_6O isomers (propylene oxide, propanal, and acetone). The proposed chemical kinetic mechanism yields qualitative agreement with the measurements. Very recently, Veloo et al.[32] conducted JSR and flame studies on the oxidation of propanal over a wide range of equivalence ratios, temperatures, and ambient pressures. A detailed model covering low- and high-temperature kinetics was proposed and validated against the JSR, flame speed, and ignition delay data. For the oxidation of *n*-butanal, only Davidson et al.[33] measured its ignition delay times behind reflected shock waves at ϕ = 0.5 and 1.0 and pressures of 1.4 and 2.6 atm. da Silva et al.[34] calculated the enthalpies of formation, bond dissociation energies (BDEs), and molecular structures of the *n*-aldehydes (acetaldehyde, propanal, *n*-butanal, *n*-pentanal, *n*-hexanal, and *n*-heptanal) using G3, G3B3, and CBS-APNO methods. The analysis of BDEs reveals that the $R-CH_2CHO$ bond is the weakest bond in all aldehydes larger than acetaldehyde. Up to now, no fundamental experiments or calculations were reported on the oxidation of isobutanal. Thus, an experimental study and mechanism optimization on the oxidation of isobutanal are worthwhile.

In this study, ignition delay times of isobutanal were measured behind reflected shock waves over a wide range of equivalence ratios, temperatures, and pressures. An improved isobutanal submodel was given on the basis of literature review and validated against the experimental results.

2. EXPERIMENTAL SECTION

Measurements were carried out in a shock tube with 11.5 cm inner diameter. It is separated into a 4.0 m long driver section and a 4.8 m long driven section by double polyester terephthalate (PET) diaphragms. Details of the shock tube were presented elsewhere.[35,36] Fuel mixtures were prepared manometrically in a 128 L stainless-steel tank and allowed to mix for at least 12 h by molecular diffusion. To

Received: December 25, 2012
Revised: April 3, 2013
Published: April 3, 2013

dx.doi.org/10.1021/ef302164n | Energy Fuels 2013, 27, 2804−2810

minimize the possibility of fuel condensation, the partial pressure of liquid fuel is kept below 50% of its corresponding saturation vapor pressure at room temperature. The purities of liquid isobutanal, argon, oxygen, and helium are 99.5, 99.995, 99.995, and 99.999%, respectively. The ignition delay time is defined as the time interval between the arrival of the incident shock wave at the endwall and the extrapolation of the steepest rise in the endwall OH* chemiluminescence signal to the zero baseline, as shown in Figure 1. The

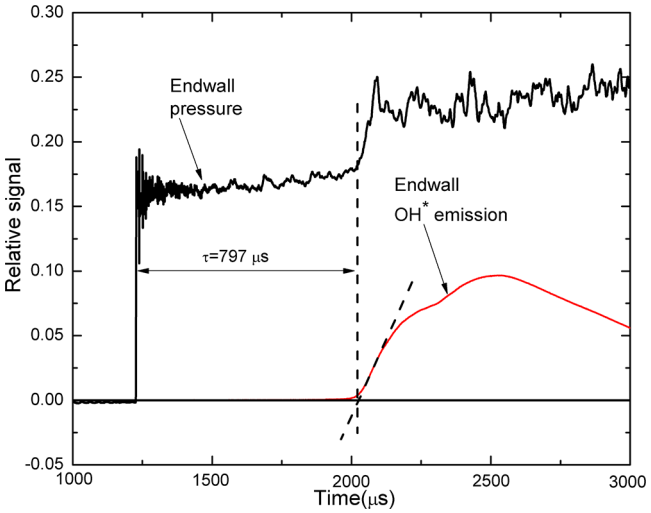

Figure 1. Typical endwall pressure and OH* chemiluminescence measurements with corresponding ignition delay time for stoichiometric 0.6% isobutanal at 4.98 atm and 1278 K (the extrapolation of the steepest rise of the OH* chemiluminescence is represented by a dashed line).

incident shock velocity at the endwall is determined by linear extrapolation of three time intervals recorded by three time counters (Fluke, PM6690). The OH* chemiluminescence selected by a narrow filter centered at 306 ± 10 nm is measured with a photomultiplier (Hamamatsu, CR131) located at the endwall. All data were recorded using a digital recorder (Yokogawa, ScopeCorder DL750). The temperature behind the reflected shock wave was calculated using the reflected shock module in the software Gaseq.[37] The uncertainty of the temperatures is about ±25 K. The Chemkin II[38] software was employed to calculate the ignition delay times. The calculated ignition delay time was obtained as the beginning of the simulation to the time having the maximum temperature rise. As discussed in the previous study,[35] the non-ideal effect is very limited for the high-temperature measurement in the shock tube. Therefore, the pressure rise was not considered in the simulation because of the relatively short ignition delay times (less than 1.5 ms) and high dilution with argon.

The experiments were performed at equivalence ratios of 0.5, 1.0, and 2.0, pressures of 1.3−10 atm, and temperatures of 1100−1650 K. Composition of the fuel/oxygen/argon mixture is given in Table 1. Most of the mixtures were prepared at a dilution level of ~95%, except for one series, which has a dilution of 85%.

3. KINETIC MODELING

The improved isobutanal submodel was developed on the basis of the C_4 chemistry[39] proposed by the Curran group. It is noted that, except the isobutanal submodel, the main C_4 mechanism was employed without any modification. In the improved submodel, reactions of isobutanal were added or modified on the basis of literature values. The thermodynamic data of isobutanal and the relevant radicals in the C_4 model were consistently inherited in the improved model. The added CH_3CHCHO chemistry was derived from Akih-Kumgeh et al.[29] The details of the submodel are provided in Table 2. The

Table 1. Mixture Compositions in This Study

isobutanal (%)	O_2 (%)	ϕ	p_5 (atm)
1.2	3.3	0.5	1.3
1.2	6.6	1.0	1.3
1.2	13.2	2.0	1.3
0.6	1.65	0.5	5
0.6	3.3	1.0	5
0.6	6.6	2.0	5
0.6	1.65	0.5	10
0.6	3.3	1.0	10
0.6	6.6	2.0	10

complete mechanism is available as Supporting Information or from the authors.

3.1. Unimolecular Decomposition. Four unimolecular decomposition reactions are included in the improved submodel.

$$IC_3H_7CHO \Leftrightarrow IC_3H_7 + HCO \quad \text{(R1307)}$$

$$IC_3H_7CHO \Leftrightarrow CH_3 + CH_3CHCHO \quad \text{(R1308)}$$

$$IC_3H_7CHO \Leftrightarrow IC_3H_7CO + H \quad \text{(R1309)}$$

$$IC_3H_7CHO \Leftrightarrow (CH_3)_2CCHO + H \quad \text{(R1310)}$$

The rate constants for reactions R1307−R1310 were calculated from microscopic reversibility using an estimate of the rate constant for radical−radical recombination. This method was also employed by Johnson et al.[40] and Black et al.[41] for the decomposition of propanol and *n*-butanol, respectively. For reaction R1307, a rate constant of 1.806×10^{13} cm^3 mol^{-1} s^{-1} was used as recommended by Tsang[42] for formyl radical recombination with isopropyl radical. Reaction R1308 was estimated to be $1.368 \times 10^{15} \times T^{-0.68}$ cm^3 mol^{-1} s^{-1} as recommended by Tsang[42] for the recombination of methyl and isopropyl radicals to form isobutane. For reaction R1309, the rate constant was estimated to be 1.0×10^{14} cm^3 mol^{-1} s^{-1} as recommended by Johnson et al.[40] and Black et al.[41] for hydrogen atom addition to other free radicals. The rate constant for reaction R1310 was estimated to be 2.408×10^{13} cm^3 mol^{-1} s^{-1} as recommended by Tsang[43] for hydrogen atom addition to *tert*-butyl radicals to form isobutane. Additionally, according to the rate of production (ROP) analysis of isobutanal using the C_4 model, the original rate constant for the reaction $IC_3H_7CHO + H = IC_4H_9O$ is too high. It was replaced by a rate constant of $4 \times 10^{12} \times \exp(-6.26$ kcal mol$^{-1}/RT)$ cm^3 mol^{-1} s^{-1} recommended by Curran et al.[44] for the reaction $C_2H_5CHO + H = NC_3H_7O$.

3.2. Hydrogen Abstraction. According to the study by da Silva et al.,[34] the carbon chain length or chain branching exerts little influence on the BDEs of the C−H bond in formyl and methyl groups of aldehydes larger than acetaldehyde. Therefore, an analogous method can be used to obtain the rate constants of H-abstractions. The rate constants for H-abstraction by H radicals from the formyl group and its neighboring carbon site were estimated to be $1.31 \times 10^5 \times T^{2.58}$ $\exp(-1.22$ kcal mol$^{-1}/RT)$ cm^3 mol^{-1} s^{-1} as recommended by Sivaramakrishnan et al.[45] for acetaldehyde and $1.3 \times 10^6 \times T^{2.4}$ $\times \exp(-4.47$ kcal mol$^{-1}/RT)$ cm^3 mol^{-1} s^{-1} as recommended by Veloo et al.[32] for isobutanal. For H-abstraction by OH radicals from these sites, a rate constant of $2.65 \times 10^{12} \times \exp(0.73$ kcal mol$^{-1}/RT)$ cm^3 mol^{-1} s^{-1} as recommended by Sivakumaran et al.[46] for acetaldehyde and $1.68 \times 10^{12} \times \exp(0.3$

dx.doi.org/10.1021/ef302164n | Energy Fuels 2013, 27, 2804−2810

Table 2. Improved Isobutanal Submodel[a]

number	reaction	A	n	E_a	reference
	Unimolecular Decomposition				
R1307	$IC_3H_7CHO \Leftrightarrow IC_3H_7 + HCO$	1.88×10^{24}	−2.146	83940	est. 42
R1308	$IC_3H_7CHO \Leftrightarrow CH_3 + CH_3CHCHO$	2.83×10^{19}	−1.097	79830	est. 42
R1309	$IC_3H_7CHO \Leftrightarrow IC_3H_7CO + H$	1.07×10^{17}	−0.392	89120	est.
R1310	$IC_3H_7CHO \Leftrightarrow (CH_3)_2CCHO + H$	4.26×10^{14}	−0.135	89870	est. 43
	Hydrogen Abstraction				
R1311	$IC_3H_7CHO + H \Leftrightarrow IC_3H_7CO + H_2$	1.31×10^{5}	2.58	1220	est. 45
R1312	$IC_3H_7CHO + H \Leftrightarrow (CH_3)_2CCHO + H_2$	1.30×10^{6}	2.4	4471	est. 32
R1313	$IC_3H_7CHO + H \Leftrightarrow CH_2(CH_3)CHCHO + H_2$	1.33×10^{6}	2.5	6756	est. 40
R1314	$IC_3H_7CHO + OH \Leftrightarrow IC_3H_7CO + H_2O$	2.65×10^{12}	0	−730	est. 46
R1315	$IC_3H_7CHO + OH \Leftrightarrow (CH_3)_2CCHO + H_2O$	1.68×10^{12}	0	−781	39
R1316	$IC_3H_7CHO + OH \Leftrightarrow CH_2(CH_3)CHCHO + H_2O$	1.05×10^{10}	1	1586	est. 40
R1317	$IC_3H_7CHO + HO_2 \Leftrightarrow IC_3H_7CO + H_2O_2$	3.00×10^{12}	0	11920	39
R1318	$IC_3H_7CHO + HO_2 \Leftrightarrow (CH_3)_2CCHO + H_2O_2$	1.00×10^{12}	0	14000	32
R1319	$IC_3H_7CHO + HO_2 = CH_2(CH_3)CHCHO + H_2O_2$	1.70×10^{13}	0	20440	est. 40
R1320	$IC_3H_7CHO + O_2 \Leftrightarrow IC_3H_7CO + HO_2$	4.00×10^{13}	0	37600	39
R1321	$IC_3H_7CHO + O_2 \Leftrightarrow (CH_3)_2CCHO + HO_2$	1.24×10^{14}	−0.2	43350	39
R1322	$IC_3H_7CHO + O_2 \Leftrightarrow CH_2(CH_3)CHCHO + HO_2$	4.20×10^{13}	0	52000	est. 40
R1323	$IC_3H_7CHO + CH_3 \Leftrightarrow IC_3H_7CO + CH_4$	5.01×10^{10}	0	6275.9	est. 47
R1324	$IC_3H_7CHO + CH_3 = (CH_3)_2CCHO + CH_4$	1.00×10^{11}	0	7900	32
R1325	$IC_3H_7CHO + CH_3 \Leftrightarrow CH_2(CH_3)CHCHO + CH_4$	9.04×10^{-1}	3.6	7154	est. 40
R1326	$IC_3H_7CHO + O \Leftrightarrow IC_3H_7CO + OH$	7.18×10^{12}	0	1389	39
R1327	$IC_3H_7CHO + O \Leftrightarrow (CH_3)_2CCHO + OH$	1.00×10^{13}	0	3280	32
R1328	$IC_3H_7CHO + O \Leftrightarrow CH_2(CH_3)CHCHO + OH$	9.81×10^{5}	2.4	4750	est. 40
R1329	$IC_3H_7CHO + CH_3O_2 \Leftrightarrow IC_3H_7CO + CH_3O_2H$	4.09×10^{4}	2.5	10200	est. 39
R1330	$IC_3H_7CHO + CH_3O_2 \Leftrightarrow (CH_3)_2CCHO + CH_3O_2H$	3.44×10^{12}	0.1	17880	est. 39
R1331	$IC_3H_7CHO + CH_3O_2 \Leftrightarrow CH_2(CH_3)CHCHO + CH_3O_2H$	4.76×10^{4}	2.5	16490	39
R1332	$IC_3H_7CHO + HCO \Leftrightarrow IC_3H_7CO + CH_2O$	3.98×10^{12}	0	8700	32
R1333	$IC_3H_7CHO + HCO \Leftrightarrow (CH_3)_2CCHO + CH_2O$	1.23×10^{7}	2	17420	32
R1334	$IC_3H_7CHO + HCO \Leftrightarrow CH_2(CH_3)CHCHO + CH_2O$	2.04×10^{5}	2.5	18440	est. 40
	Decomposition of First-Formed Radicals				
R1335	$IC_3H_7CO \Leftrightarrow IC_3H_7 + CO$	2.87×10^{20}	−2.2	14970	39
R1336	$IC_3H_7CO \Leftrightarrow CH_3CHCO + CH_3$	2.42×10^{13}	−0.3	22470	est. 39
R1337	$IC_3H_7CO \Leftrightarrow IC_3H_6CO + H$	4.09×10^{14}	−0.1	42410	est. 39
R1338	$CH_2(CH_3)CHCHO \Leftrightarrow C_3H_6 + HCO$	1.03×10^{15}	−0.6	23170	39
R1339	$CH_2(CH_3)CHCHO \Leftrightarrow C_2H_3CHO + CH_3$	2.42×10^{13}	−0.3	22470	39
R1340	$CH_2(CH_3)CHCHO \Leftrightarrow IC_3H_5CHO + H$	4.95×10^{12}	−0.1	31300	39
R1341	$(CH_3)_2CCHO \Leftrightarrow IC_3H_5CHO + H$	1.32×10^{14}	0	39340	39
R1342	$(CH_3)_2CCHO \Leftrightarrow IC_3H_6CO + H$	4.09×10^{14}	−0.1	42410	39
R1343	$CH_3CHCHO \Leftrightarrow C_2H_4 + HCO$	1.00×10^{12}	0	34640.5	29
R1344	$CH_3CHCHO \Leftrightarrow CH_3CHCO + H$	1.67×10^{13}	0	46222	29
R1345	$CH_3CHCHO \Leftrightarrow CH_3 + CH_2CO$	6.02×10^{15}	0	14064	29

[a]Units: cm, mol, s, cal, K, and $k = AT^n \exp(E_a/RT)$.

kcal mol^{-1}/RT) cm^3 mol^{-1} s^{-1} from the C_4 model were adopted in the improved model. Rate constants of H-abstraction by H and OH radicals from the methyl groups of isopropanol used by Johnson et al.[41] were employed for those of isobutanal. Actually, in the study by Johnson et al., the rate constants for H-abstraction from the methyl group were taken to be identical to those of alkanes. In the improved model, similar approaches were performed on the H-abstractions by other radicals (HO_2, O, O_2, CH_3, HCO, and CH_3O_2). Their references were given in the last column of Table 2.

3.3. Radical Decomposition. Radical decomposition reactions were mainly derived from the C_4 model, with only some reactions (R1336, R1337, and R1340) added.

$$IC_3H_7CO \Leftrightarrow CH_3CHCO + CH_3 \quad \text{(R1336)}$$

$$IC_3H_7CO \Leftrightarrow IC_3H_6CO + H \quad \text{(R1337)}$$

$$CH_2(CH_3)CHCHO \Leftrightarrow IC_3H_5CHO + H \quad \text{(R1340)}$$

The rate constants of reactions R1366 and R1367 were estimated to be identical to that of reaction R1339 [$CH_2(CH_3)$-$CHCHO \Leftrightarrow C_2H_3CHO + CH_3$] and R1342 [$(CH_3)_2CCHO \Leftrightarrow IC_3H_6CO + H$], respectively. The rate constant of reaction R1340 was obtained on the basis of an analogy of the reaction (C_3H_6CHO-2 $\Leftrightarrow SC_3H_5CHO + H$) in the C_4 model. The added reaction pathway (R1308: $IC_3H_7CHO \Leftrightarrow CH_3 + CH_3CHCHO$), which is not included in the C_4 model, brings in a new species, CH_3CHCHO. Its chemistry was obtained from the propanal study by Akih-Kumgeh et al.[29]

4. RESULTS AND DISCUSSION

In this section, the new measured data and simulation results using the improved isobutanal submodel were first compared,

dx.doi.org/10.1021/ef302164n | Energy Fuels 2013, 27, 2804−2810

followed by the reaction pathway and sensitivity analysis of the new model. All measured data was presented in Table 3.

Table 3. Ignition Delay Times for Isobutanal

p (atm)	T (K)	τ_{ign} (μs)	p (atm)	T (K)	τ_{ign} (μs)
ϕ = 0.5, 1.2% isobutanal			10.08	1363	76
1.3	1326	158	10.25	1306	127
1.37	1377	93	10.43	1269	198
1.41	1411	68	10.37	1227	352
1.32	1351	122	9.81	1174	565
1.3	1293	227	9.81	1129	934
1.23	1251	375	10.07	1103	1246
1.28	1236	436	10.19	1216	389
1.25	1186	694	10.31	1243	259
1.26	1212	565	ϕ = 1.0, 0.6% isobutanal		
1.25	1164	847	5.2	1424	161
1.24	1133	1246	5.16	1382	262
ϕ = 1.0, 1.2% isobutanal			5.24	1354	347
1.32	1371	279	5.17	1312	558
1.38	1297	527	4.98	1278	797
1.32	1452	138	5.09	1233	1189
1.27	1401	214	5.31	1484	96
1.38	1493	94	5.19	1448	143
1.3	1316	471	4.95	1517	65
1.27	1326	414	10.2	1431	92
1.26	1271	711	9.96	1351	218
1.26	1247	900	10.15	1319	328
1.29	1511	78	10.43	1409	140
1.29	1345	368	10.01	1380	173
1.25	1281	673	10.03	1235	734
1.29	1239	939	9.68	1266	631
1.25	1281	674	10.16	1256	749
ϕ = 2.0, 1.2% isobutanal			9.89	1198	1025
1.19	1412	629	10	1314	368
1.23	1474	326	ϕ = 2.0, 0.6% isobutanal		
1.19	1530	231	5.14	1459	483
1.18	1545	205	5.25	1426	647
1.19	1587	138	5.08	1381	999
1.36	1645	97	5.19	1492	341
1.31	1647	92	5.01	1502	324
1.26	1445	503	5.22	1537	194
1.26	1495	318	5.03	1603	109
1.25	1364	914	5.14	1574	154
1.28	1361	1018	5.08	1621	94
1.22	1322	1348	5.22	1556	188
ϕ = 0.5, 0.6% isobutanal			10	1476	271
5.45	1379	80	10.2	1562	131
5.24	1340	146	10.5	1601	89
5.33	1308	206	10.33	1491	227
5.16	1268	324	10.49	1541	156
5.12	1230	495	10	1371	760
5.24	1211	609	10.23	1428	442
5.18	1177	908	10.25	1393	554
5.06	1146	1366	10.05	1340	913
5.37	1409	63			

4.1. Comparison between Experimental and Modeling Results. The simulation of ignition delay times was performed using Chemkin II[38] in a constant-volume, adiabatic, and zero-dimensional reactor. The original C_4 model[39] and Veloo model[32] were also used for comparison. It is noted that the C_4 model primarily aims at C_1−C_4 alkanes, including only a rough isobutanal submodel. The Veloo model focuses on the oxidation of propanal, with a detailed isobutanal model included. However, both of these isobutanal models have not yet been validated against experimental results.

Figures 2−4 give the comparison between experimental and modeling results at various pressures and equivalence ratios. At p = 1.3 atm, the improved model yields fairly good agreement with the experimental data but slight overprediction at a low temperature and slight underprediction at a high temperature, leading to a higher simulated activation energy. The Veloo model also gives fairly good prediction at three different equivalence ratios. However, remarkable overprediction occurs in the low-temperature range under fuel-lean conditions. The C_4 model yields large underprediction at all three equivalence ratios. At p = 5.0 and 10.0 atm, the improved model also yields fairly good prediction under different equivalence ratios. However, the Veloo model vastly overpredicts the ignition delay times at all equivalence ratios and shows higher activation energies. Similar to the simulation results at p = 1.3 atm, the C_4 model yields quite notable underprediction at 5.0 and 10.0 atm at all equivalence ratios.

4.2. Reaction Pathway Analysis. Figure 5 shows the instantaneous analysis on reaction pathways for a 1.2% isobutanal mixture at p = 1.3 atm, T = 1400 K, and ϕ = 1.0. The timing of 20% fuel consumption is chosen for the analysis, which is the same as that in the literature.[17,35]

Under this condition, the unimolecular decomposition and H-abstraction reactions totally contribute to the fuel consumption by 17 and 83%, respectively. Among these unimolecular decomposition reactions, the breakage of the R−CHO bond is the dominant pathway (15.1%) and produces isopropyl and formyl radicals, while the breakage of the CH_3−R bond only consumes 2% of the isobutanal to form methyl and CH_3CHCHO radicals. In fact, in the temperature range of this study, these two decomposition reactions have very close rate constants. The quite low branching ratio of the latter pathway is ascribed to the higher concentration of methyl radicals. The methyl radicals are mainly produced by reactions $CH_2(CH_3)$-$CHCHO \Leftrightarrow C_2H_3CHO + CH_3$, $IC_3H_7CHO \Leftrightarrow CH_3 + CH_3CHCHO$, and $CH_3CHCHO \Leftrightarrow CH_3 + CH_2CO$ and consumed by reactions $CH_3 + HO_2 \Leftrightarrow CH_3O + OH$, $2CH_3 (+M) \Leftrightarrow C_2H_6 (+M)$, etc. The rate of production of methyl radicals is much faster than the rate of its consumption. The accumulation of methyl radicals facilitates the reverse reaction rate of the latter decomposition pathway and, consequently, decreases the branching ratio of this pathway. The other three radicals have a very slow net rate of production and relatively much lower concentrations. Two other possible unimolecular decomposition reactions [$IC_3H_7CHO \Leftrightarrow IC_3H_7CO + H$ and $IC_3H_7CHO \Leftrightarrow (CH_3)_2CCHO + H$] were included in the improved model, but they had negligible contribution to fuel consumption and were not presented in Figure 5. H-abstraction reactions from three different carbon sites have comparable branching ratios. Specifically, H-abstraction by H radicals plays a dominant role at three different carbon sites compared to other radicals, which is probably because of the relatively high H radical mole fraction during the oxidation of isobutanal. For the first-formed radicals [IC_3H_7CO, $CH_2(CH_3)CHCHO$, and $(CH_3)_2CCHO$], the IC_3H_7CO radical mainly decomposes to form IC_3H_7 and CO. This is similar to the decomposition of the C_2H_5CO radical in the propanal model proposed by Veloo et al.[32] In their study, it is the dominant pathway at both high and low temperatures. The formed ethyl radicals then undergo

dx.doi.org/10.1021/ef302164n | Energy Fuels 2013, 27, 2804−2810

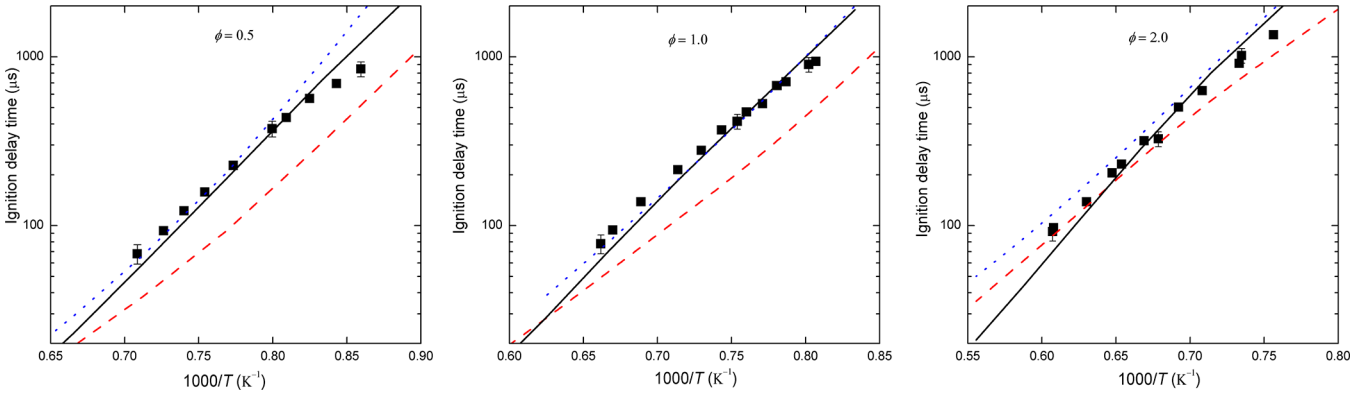

Figure 2. Comparison between experimental and modeling results at p = 1.3 atm for 1.2% isobutanal (symbols, experimental data; dashed line, C_4 model; dotted line, Veloo model; and solid line, improved model).

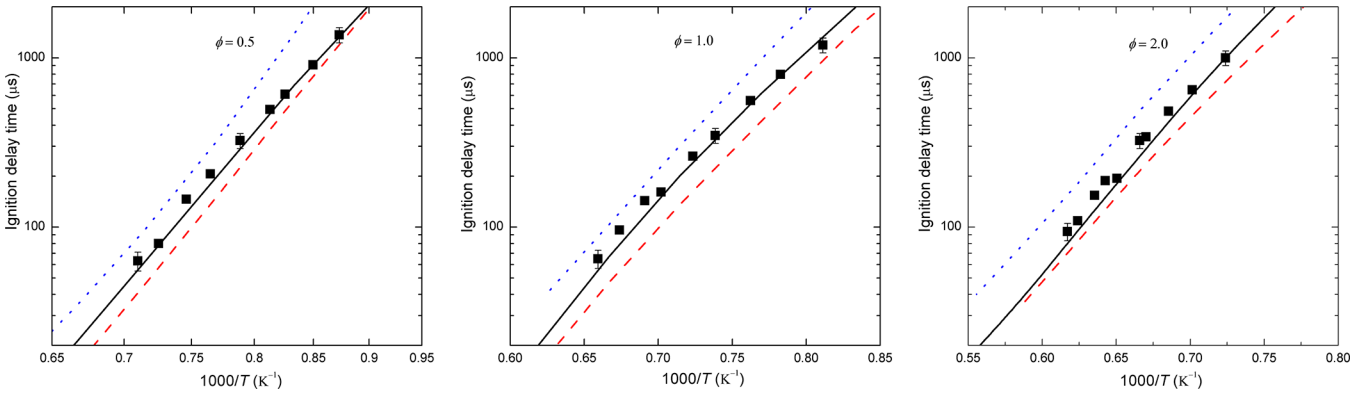

Figure 3. Comparison between experimental and modeling results at p = 5.0 atm for 0.6% isobutanal (symbols, experimental data; dashed line, C_4 model; dotted line, Veloo model; and solid line, improved model).

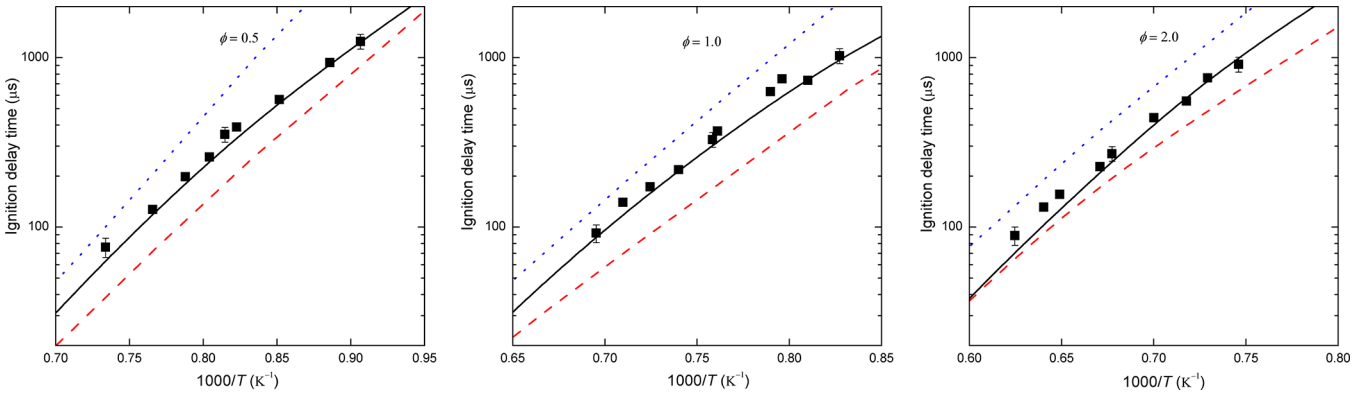

Figure 4. Comparison between experimental and modeling results at p = 10.0 atm for 0.6% isobutanal (symbols, experimental data; dashed line, C_4 model; dotted line, Veloo model; and solid line, improved model).

low-temperature chain branching at a low temperature, leading to the appearance of a cool flame. Therefore, it can be inferred that this pathway is also of great importance for the oxidation of isobutanal at a low temperature. The other two pathways ($IC_3H_7CO \Leftrightarrow CH_3CHCO + CH_3$ and $IC_3H_7CO \Leftrightarrow IC_3H_6CO + H$) for the consumption of IC_3H_7CO radicals were not presented in Figure 5 for their tiny contribution (less than 0.5%). There are two pathways for the decomposition of the $(CH_3)_2CCHO$ radical. Both of them proceed through β-scission with the breakage of C−H bonds. The favored pathway of the decomposition of the $CH_2(CH_3)CHCHO$ radical is to yield propene and formyl radical with a percentage of 72.1%, while another pathway is to yield C_2H_3CHO and methyl radical with a percentage of 27.5%.

4.3. Sensitivity Analysis. To ascertain the important reactions, a sensitivity analysis was performed under a selected condition where the improved model still yields relatively poor prediction. The normalized sensitivity is defined as

$$S = \frac{\tau(2k_i) - \tau(0.5k_i)}{1.5\tau(k_i)} \quad (1)$$

where τ is the ignition delay time and k_i is the pre-exponential factor of the ith reaction. A negative coefficient indicates a promoting effect on the overall reactivity and vice versa.

dx.doi.org/10.1021/ef302164n | Energy Fuels 2013, 27, 2804−2810

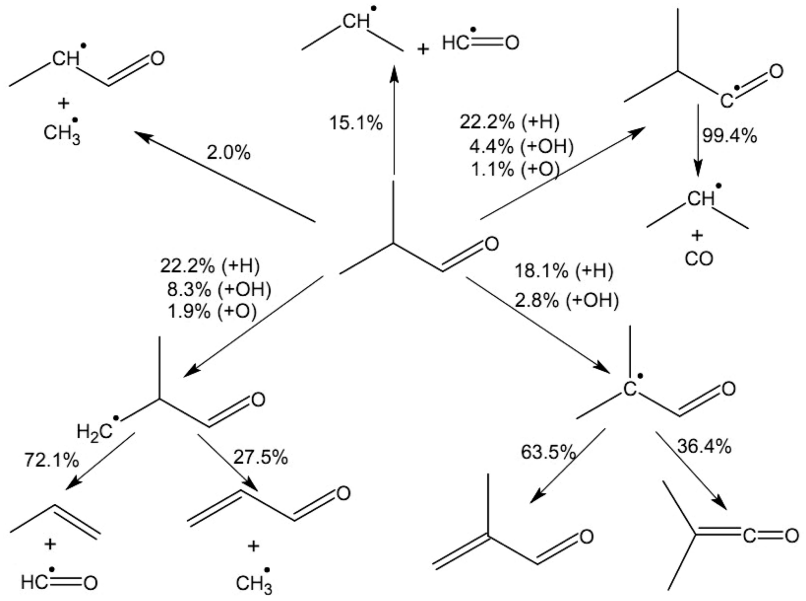

Figure 5. Reaction pathway diagram of the improved model for 1.2% isobutanal in a shock tube at p = 1.3 atm, T = 1400 K, ϕ = 1.0, and 20% fuel consumption.

As shown in Figure 2, the improved model slightly overpredicts the ignition delay time at a low temperature and underpredicts it at a high temperature. Therefore, the sensitivity analysis was performed at two temperatures, as shown in Figure 6. For a low temperature, T = 1200 K, reaction R1 exhibits high

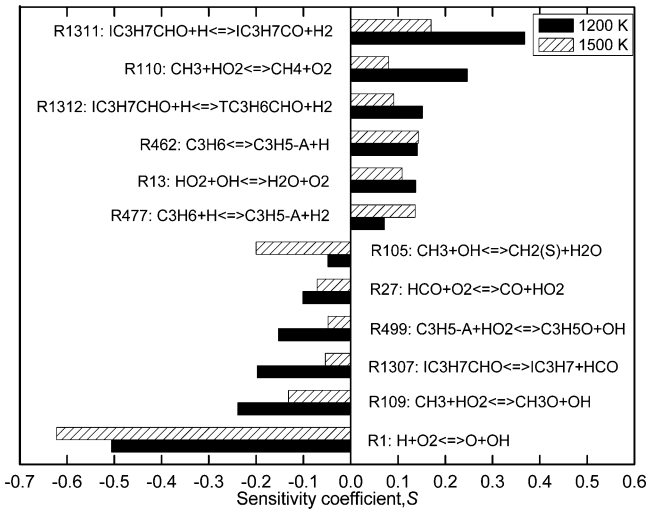

Figure 6. Sensitivity analysis for 1.2% isobutanal at T = 1200 and 1500 K, p = 1.3 atm, and ϕ = 1.0.

sensitivity as well as some other reactions involving small radicals (R109, R110, etc.). Three fuel-specific reactions (R1307, R1311, and R1312) are also presented among the 12 most sensitive reactions. Particularly, the sensitivities of reactions R1307 and R1311 at T = 1200 K are higher than those at T = 1500 K. As a result, an appropriate decrease in the rate constant of reaction R1311 combined with an increase in the rate constant of reaction R1307 could reduce the simulated ignition delay times, leading to better agreement with the measured data at a low temperature. For a high temperature, T = 1500 K, reaction 1 also has the highest sensitivity. In addition, the ignition delay time is relatively more sensitive to the small radical reactions. However, any modification on small radial reactions may worsen the model performance for other fuels. As mentioned above, the improved model employed the C_0–C_4 chemistry of the C_4 model (except the isobutanal submodel) without any modification. Therefore, further specific experiments or high-level theoretical calculations on these sensitive fuel-specific reactions are needed to improve the model.

5. CONCLUSION

Ignition delay times of isobutanal were measured over a wide range of equivalence ratios, pressures, and temperatures. A detailed isobutanal submodel was developed on the basis of literature review. In comparison to the previous isobutanal models, the improved model shows notable improvements on the prediction of ignition delay times under all measured conditions. Analysis on reaction pathways shows that the breakage at the R–CHO bond is the dominant pathway for unimolecular decomposition reactions. For H-abstractions, the abstraction by H radical plays a dominant role at all sites. Sensitivity analysis was performed under selected conditions to ascertain the important reactions for modeling improvement. To further optimize the isobutanal model, accurate calculations on the BDEs of isobutanal and rate constants of unimolecular decomposition and H-abstraction reactions, as well as validation against other experimental targets (e.g., JSR or flames), are recommended.

■ ASSOCIATED CONTENT

Supporting Information

C_4 chemistry by the Curran group and thermochemistry derived from the C_4 model by the Curran group. This material is available free of charge via the Internet at http://pubs.acs.org.

■ AUTHOR INFORMATION

Corresponding Author

*Telephone: +86-29-82665075. Fax: +86-29-82668789. E-mail: zhhuang@mail.xjtu.edu.cn.

Notes

The authors declare no competing financial interest.

■ ACKNOWLEDGMENTS

This work is supported by the National Natural Science Foundation of China (Grants 51136005 and 51121092) and the National Basic Research Program (2013CB228406).

■ REFERENCES

(1) Nigam, P. S.; Singh, A. *Prog. Energy Combust. Sci.* **2011**, *37* (1), 52−68.
(2) Harvey, B. G.; Meylemans, H. A. *J. Chem. Technol. Biotechnol.* **2011**, *86* (1), 2−9.
(3) Alasfour, F. N. *Appl. Therm. Eng.* **1998**, *18* (5), 245−256.
(4) Alasfour, F. N. *Appl. Therm. Eng.* **1998**, *18* (8), 609−618.
(5) Irimescu, A. *Int. Commun. Heat Mass Transfer* **2010**, *37* (9), 1203−1207.
(6) Irimescu, A. *Appl. Energy* **2012**, *96*, 477−483.
(7) Al-Hasan, M. I.; Al-Momany, M. *Transport* **2008**, *23* (4), 306−310.
(8) Karabektas, M.; Hosoz, M. *Renewable Energy* **2009**, *34* (6), 1554−1559.
(9) McEnally, C. S.; Pfefferle, L. D. *Proc. Combust. Inst.* **2005**, *30* (1), 1363−1370.
(10) Yang, B.; Oßwald, P.; Li, Y.; Wang, J.; Wei, L.; Tian, Z.; Qi, F.; Kohse-Höinghaus, K. *Combust. Flame* **2007**, *148* (4), 198−209.
(11) Moss, J. T.; Berkowitz, A. M.; Oehlschlaeger, M. A.; Biet, J.; Warth, V.; Glaude, P. A.; Battin-Leclerc, F. *J. Phys. Chem. A* **2008**, *112* (43), 10843−10855.
(12) Togbé, C.; Mzé-Ahmed, A.; Dagaut, P. *Energy Fuels* **2010**, *24* (9), 5244−5256.
(13) Welz, O.; Savee, J. D.; Eskola, A. J.; Sheps, L.; Osborn, D. L.; Taatjes, C. A. *Proc. Combust. Inst.* **2013**, *34* (1), 493−500.
(14) Gu, X.; Huang, Z.; Wu, S.; Li, Q. *Combust. Flame* **2010**, *157* (12), 2318−2325.
(15) Grana, R.; Frassoldati, A.; Faravelli, T.; Niemann, U.; Ranzi, E.; Seiser, R.; Cattolica, R.; Seshadri, K. *Combust. Flame* **2010**, *157* (11), 2137−2154.
(16) Sarathy, S. M.; Vranckx, S.; Yasunaga, K.; Mehl, M.; Oßwald, P.; Metcalfe, W. K.; Westbrook, C. K.; Pitz, W. J.; Kohse-Höinghaus, K.; Fernandes, R. X.; Curran, H. J. *Combust. Flame* **2012**, *159* (6), 2028−2055.
(17) Yasunaga, K.; Mikajiri, T.; Sarathy, S. M.; Koike, T.; Gillespie, F.; Nagy, T.; Simmie, J. M.; Curran, H. J. *Combust. Flame* **2012**, *159* (6), 2009−2027.
(18) Vardanyan, I. A.; Sachyan, G. A.; Nalbandyan, A. B. *Combust. Flame* **1971**, *17* (3), 315−322.
(19) Vardanyan, I. A.; Sachyan, G. A.; Philiposyan, A. G.; Nalbandyan, A. B. *Combust. Flame* **1974**, *22* (2), 153−159.
(20) Dean, A. M.; Johnson, R. L.; Steiner., D. C. *Combust. Flame* **1980**, *37*, 41−62.
(21) Kaiser, E. W.; Westbrook, C. K.; Pitz, W. J. *Int. J. Chem. Kinet.* **1986**, *18* (6), 655−688.
(22) Dagaut, P.; Reuillon, M.; Voisin, D.; Cathonnet, M.; McGuinness, M.; Simmie, J. M. *Combust. Sci. Technol.* **1995**, *107* (4−6), 301−316.
(23) Yasunaga, K.; Kubo, S.; Hoshikawa, H.; Kamesawa, T.; Hidaka, Y. *Int. J. Chem. Kinet.* **2008**, *40* (2), 73−102.
(24) Salooja, K. C. *Combust. Flame* **1965**, *9* (4), 373−382.
(25) Baldwin, R. R.; Langford, D. H.; Matchan, M. J.; Walker, R. W.; Yorke, D. A. *Proc. Combust. Inst.* **1971**, *13* (1), 251−259.
(26) Baldwin, R. R.; Lewis, K. A.; Walker, R. W. *Combust. Flame* **1979**, *34*, 275−283.
(27) Kaiser, E. *Int. J. Chem. Kinet.* **1987**, *19* (5), 457−486.
(28) Lifshitz, A.; Tamburu, C.; Suslensky, A. *J. Phys. Chem.* **1990**, *94* (7), 2966−2972.
(29) Akih-Kumgeh, B.; Bergthorson., J. M. *Combust. Flame* **2011**, *158* (10), 1877−1889.
(30) Kasper, T.; Struckmeier, U.; Oßwald, P.; Kohse-Höinghaus, K. *Proc. Combust. Inst.* **2009**, *32* (1), 1285−1292.
(31) Burluka, A. A.; Harker, M.; Osman, H.; Sheppard, C. G. W.; Konnov, A. A. *Fuel* **2010**, *89* (10), 2864−2872.
(32) Veloo, P. S.; Dagaut, P.; Togbe, C.; Dayma, G.; Sarathy, S. M.; Westbrook, C. K.; Egolfopoulos, F. N. *Proc. Combust. Inst.* **2012**, *34* (1), 599−606.
(33) Davidson, D. F.; Ranganath, S. C.; Lam, K. Y.; Liaw, M.; Hong, Z.; Hanson, R. K. *J. Propul. Power* **2010**, *26* (2), 280−287.
(34) da Silva, G.; Bozzelli, J. W. *J. Phys. Chem. A* **2006**, *110* (48), 13058−13067.
(35) Zhang, J.; Wei, L.; Man, X.; Jiang, X.; Zhang, Y.; Hu, E.; Huang, Z. *Energy Fuels* **2012**, *26* (6), 3368−3380.
(36) Zhang, J.; Niu, S.; Zhang, Y.; Tang, C.; Jiang, X.; Hu, E.; Huang, Z. *Combust. Flame* **2013**, *160* (1), 31−39.
(37) Morley, C. *Gaseq, Version 0.76*; http://www.gaseq.co.uk.
(38) Kee, R. J.; Rupley, F. M.; Miller, J. A. *Chemkin-II: A Fortran Chemical Kinetics Package for the Analysis of Gas-Phase Chemical Kinetics*; Sandia National Laboratories: Albuquerque, NM, 1989; SAND89-8009.
(39) Bourque, G.; Healy, D.; Curran, H. J.; Zinner, C.; Kalitan, D.; de Vries, J.; Aul, C.; Petersen, E. *Proc. ASME Turbo Expo: Power Land, Sea, Air* **2008**, 1051−1066.
(40) Johnson, M. V.; Goldsborough, S. S.; Serinyel, Z.; O'Toole, P.; Larkin, E.; O'Malley, G.; Curran, H. J. *Energy Fuels* **2009**, *23*, 5886−5898.
(41) Black, G.; Curran, H. J.; Pichon, S.; Simmie, J. M.; Zhukov, V. *Combust. Flame* **2010**, *157* (2), 363−373.
(42) Tsang, W. *J. Phys. Chem. Ref. Data* **1988**, *17* (2), 887−951.
(43) Tsang, W. *J. Phys. Chem. Ref. Data* **1990**, *19* (1), 1−68.
(44) Curran, H. J. *Int. J. Chem. Kinet.* **2006**, *38* (4), 250−275.
(45) Sivaramakrishnan, R.; Michael, J. V.; Klippenstein, S. J. *J. Phys. Chem. A* **2009**, *114* (2), 755−764.
(46) Sivakumaran, V.; Crowley, J. N. *Phys. Chem. Chem. Phys.* **2003**, *5* (1), 106−111.
(47) Peter, G.; Acs, A.; Horvath, I.; Huhn, P. *Acta Chim. Hung.* **1981**, *108*, 235−248.